JMEPEG (2014) 23:1157–1164
DOI: 10.1007/s11665-014-0922-y

1059-9495/$19.00

Microstructure and Properties of SAE 2205 Stainless Steel After Salt Bath Nitrocarburizing at 450 °C

Jing Yan, Jun Wang, Yuanhua Lin, Tan Gu, Dezhi Zeng, Runbo Huang, Xiong Ji, and Hongyuan Fan

(Submitted September 17, 2012; in revised form January 27, 2014; published online February 26, 2014)

Nitrocarburizing of the type SAE 2205 duplex stainless steel was conducted at 450 °C, using a type of salt bath chemical surface treatment, and the microstructure and properties of the nitrided surface were systematically researched. Experimental results revealed that a modified layer transformed on the surface of samples with the thickness ranging from 3 to 28 μm changed with the treatment time. After 2205 duplex stainless steel was subjected to salt bath nitriding at 450 °C for time less than 8 h, the preexisting ferrite zone in the surface transformed into austenite by active nitrogen diffusion. The main phase of the nitrided layer was the expanded austenite. When the treatment time was extended to 16 h, the preexisting ferrite zone in the expanded austenite was decomposed and transformed partially into ε-nitride precipitate. When the treatment time extended to 40 h, the preexisting ferrite zone in the expanded austenite was transformed into ε-nitride and CrN precipitate. Further, a large amount of nitride precipitated from preexisting austenite zone. The nitrided layer depth thickness changed intensively with the increasing nitriding time. The growth of the nitride layer takes place mainly by nitrogen diffusion according to the expected parabolic rate law. The salt bath nitriding can effectively improve the surface hardness. The maximum values measured from the treated surface are observed to be approximately 1400 $HV_{0.1}$ after 8 h, which is about 3.5 times as hard as the untreated material (396 $HV_{0.1}$). Low-temperature nitriding can improve the erosion/corrosion resistance. After nitriding for 4 h, the sample has the best corrosion resistance.

Keywords erosion/corrosion, SAE 2205 stainless steel, salt bath nitrocarburizing, microhardness, microstructure

1. Introduction

Nowadays, with excellent corrosion resistance and shock resistance, duplex stainless steel (DSS) is widely used in petrochemical, chemical, and food plants. The DSS microstructure consists of austenitic and ferritic grains balanced to approximately equal amounts under solution-annealed condition. It is also considered the enhancement of austenitic stainless steel, especially when high corrosion resistance is required (Ref 1-4). However, the low surface hardness and poor wear and fatigue resistance have restricted their applications (Ref 5-9). Nitriding is an efficient process for improving the surface hardness and anti-wear properties of stainless steel (Ref 10-14).

Jing Yan, School of Manufacturing Science and Engineering, Sichuan University, Chengdu 610065, People's Republic of China; and Southwest Oil and Gasfield Company Research Institute of Natural Gas, Chengdu 610023, People's Republic of China; **Jun Wang, Runbo Huang, Xiong Ji,** and **Hongyuan Fan**, School of Manufacturing Science and Engineering, Sichuan University, Chengdu 610065, People's Republic of China; **Yuanhua Lin** and **Dezhi Zeng**, State Key Lab of Oil and Gas Reservoir Geology and Exploitation, Southwest Petroleum University, Chengdu 610500, People's Republic of China; and **Tan Gu**, Southwest Oil and Gasfield Company Research Institute of Natural Gas, Chengdu 610023, People's Republic of China. Contact e-mail: srwangjun@163.com.

Compared to the conventional gasnitriding, the salt bath nitrocarburizing, also called as "liquid nitrocarburizing" or "salt bath nitriding," was regarded as an effective, low-cost method with many advantages, such as low treatment temperature, short treatment time, high degree of shape and dimensional stabilities, and reproducibility (Ref 15-18). It is well known that the molten salt bath nitriding process is considered as an effective engineering technology to improve corrosion properties of alloy steel (Ref 19, 20). So Funatani (Ref 14) insisted that it is an environment-friendly process; and a combination of high fatigue resistance, good wear and corrosion resistance can be achieved. It can be applicable to the hardening of the high alloy steels with high reaction efficiency (Ref 21).

Stainless steel is known as a material difficult to nitriding. The passive oxide film formed on these alloys will impede the uptake and diffusion of some elements (Ref 21-23). Some ordinary salt bath nitrocarburizing techniques (above 580 °C) can boost the microhardness and wear properties of stainless steel, but lose the paramount good corrosion resistance of the alloy (Ref 21). Fortunately, some reports indicated that the "Palsonite" technology from Japan greatly improved the wear performance without impairing the corrosion resistance of stainless steel (Ref 14). Recently, the authors conducted salt bath nitrocarburizing AISI 321 and 304 stainless steels at 430 °C and found that the low-temperature salt bath nitrocarburizing improved the hardness and advanced the corrosion resistance of stainless steel (Ref 24, 25).

Unfortunately, there is insufficient knowledge about the nature of microstructure and property changes when complex salt bath nitriding is done on a duplex stainless steel at low temperature. Therefore, the aim of the study is to investigate the effect of salt bath nitrocarburizing on surface microstructure

and properties of SAE 2205 duplex stainless steels, by x-ray diffraction (XRD), microhardness, scanning electron microscopy (SEM), transmission electron microscopy (TEM), and erosion/corrosion resistance experiments.

2. Experiment

The material under investigation was a duplex 2205 stainless steel (22.7 % Cr, 5.7 % Ni, 2.57 % Mo, 1.37 % Mn, 0.38 % Si, 0.032 % P, 0.03 % C, 0.001 % S, in mass fraction). The specimens were cut from a hot rolled steel plate with the depth of 2.5 mm and then cut into 25 × 25 mm. After samples were pretreated by derusting and degreasing, the samples of DSS 2205 stainless steel were dipped in the molten salt to nitride at 450 °C for different hours and then cooled in air to room temperature. Following the heat chemical treatment, samples were ultrasonically cleaned in alcohol for 15 min.

The nitrocarburizing medium for DSS 2205 samples was a kind of salt, which mainly composed of the nontoxic M_2CO_3 (M denotes some elements of halogen), $CO(NH_2)_2$ and some trace components. The CNO^- concentration in the salt was above 40 %. The amount of remaining CN^-, which is toxic, in the waster slag is less than 0.5 %. The pretreatment to remove passive film of the steel samples was not necessary because the CNO^- in a salt bath has a strong reducing potential. The treatment temperature was 450 °C.

The structural changes in the modified layer were investigated using the cross sections by optical microscopy of BX41-72H02. The x-ray diffractometer type Dmax-1400 with Cu K-alpha radiation and a nickel filter was used to determine the phases present in the modified layer. Cross sections of the nitrocarburizing specimens were also prepared by the standard process for TEM studies in a JEOL-JEM 2010 operating at 200 kV.

Erosion/corrosion tests were performed by high-speed spinning the untreated and nitrided samples in 20 vol.% H_2SO_4 water solutions with 40 mass% Al_2O_3 particles at room temperature (about 20 °C) for up to 4 h. The corresponding schematic diagram of the simple device is shown in Fig. 1. The size of the Al_2O_3 particles was between 240 and 300 μm. The distance from sample to axis center is about 125 mm and the rotation speed is 450 rpm. After a certain time interval, samples were removed from the solution. They were cleaned and dried, and then measured with a balance accurate to 0.1 mg, so that the weight loss due to corrosion was obtained. Two batches of tests were performed, and each data reported in this paper represent the average value of two tests.

3. Results and Discussion

3.1 Metallography Observed

Microstructures of specimens nitrided at 450 °C for 8, 16, and 40 h were investigated using an optical microscope. The cross-sectional microstructure produced during salt bath nitrocarburizing of SAE 2205 type stainless steel is shown in Fig. 2. A typical nitrided layer in Fig. 2a appeared as a "white layer" under light microscope. This phenomenon indicated that a proper enhancement in corrosion resistance to the harsh etchants of the modified layer was obtained by low-temperature nitrocarburizing (Ref 11). In association with the corresponding schematic diagram shown in Fig. 2, it can be observed that the boundaries of ferrite and austenite (line of dashes in Fig. 2b) in the nitrided layer disappeared and the ferrite zone transformed into an expanded austenite zone. It is well known that nitrogen stabilizes the austenite phase and so a transformation from ferrite into austenite can be expected if the amount of nitrogen in the solid solution is high enough. This transformation was confirmed by Blawert with XRD (Ref 1).

As the treatment time increases to 16 h, there is a distinguishable difference in the austenitic and ferritic zones in the nitrided layer. A dense mass of precipitates emerged in the ferrite zone. After etching, most of the ferrite subgrains were identifiably dark in appearance. Against that, the austenite subgrain and subboundary have little precipitates. The austenite zone in the nitrided layer appeared white after etching. It is indicated that the austenite has better corrosion resistance than the ferritic zone in the modified layer. The significance of the

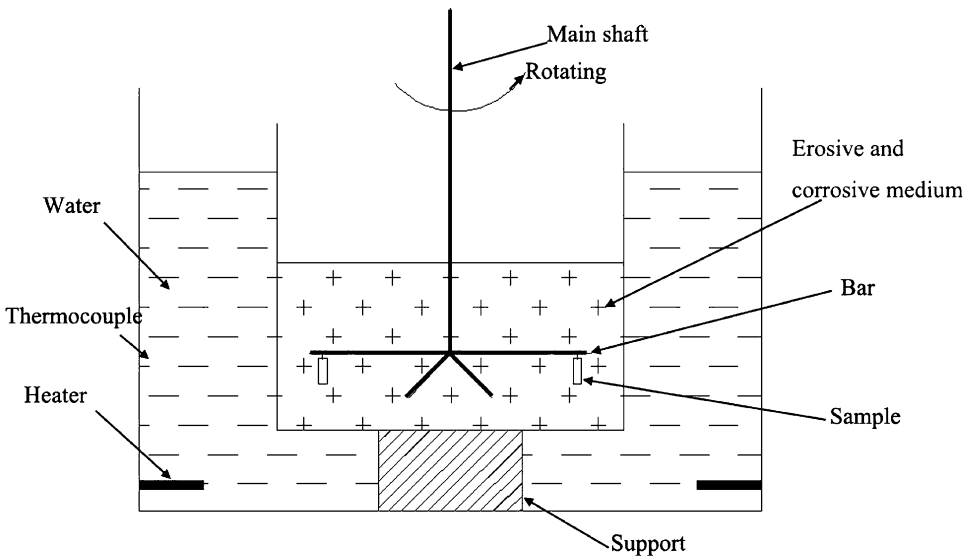

Fig. 1 Schematic diagram of erosion/corrosion tester

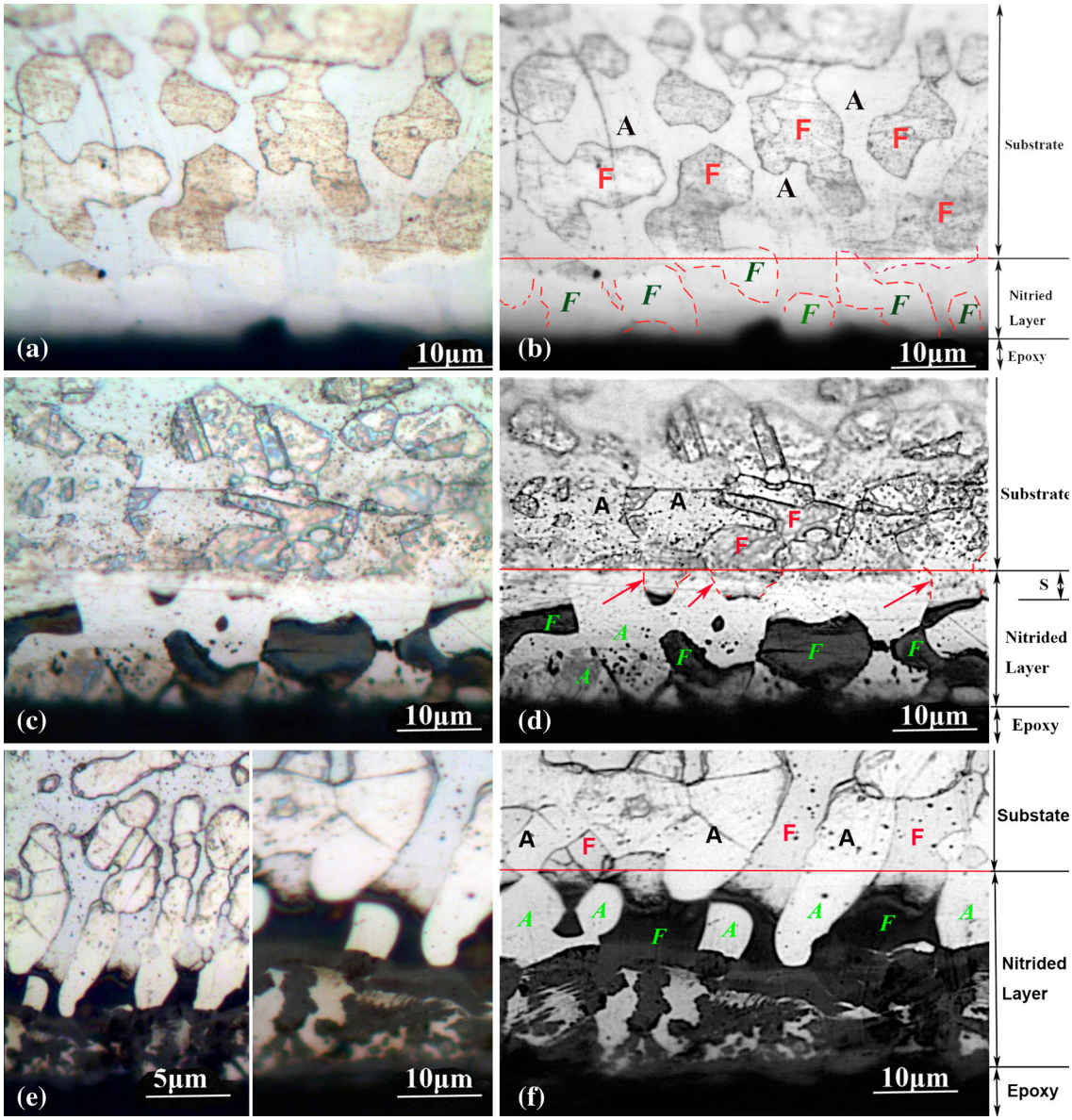

Fig. 2 Cross-sectional microstructure of sample nitrided at temperature 450 °C (a 8 h, c 16 h, e 40 h; b schematic diagram of a, d schematic diagram of c, f schematic diagram of e)

white and black microstructure shows that there are still some ferrite zones which did not have precipitated nitride (arrowed in Fig. 2d).

After salt bath nitriding for 40 h, a thicker nitrided layer was produced. It was observed that there was an increase in the amount of nitrides precipitated in the ferrite of the whole nitride layer. Comparing this result with 16 h nitridation, there is a large mass of nitride precipitates dispersed in the austenitic subgrain near the surface. The nitride precipitates were significantly increased due to a local stress concentration in the nitrided layer; and in observing the middle zone, it is apparent that a mass of nitride precipitates was dispersed in austenite subgrain, which still shows some zones having no precipitate. Although the precipitate was not shown in this zone, there were some dark nitride precipitates produced in austenitic subgrain (Fig. 2f). However, in the interior zone near the substrate, the nitride precipitates were shown only to disperse in the ferrite region, which resulted in the formation of etching tracks. Furthermore, the color of austenite subgrains does not change after etching the sample. This is due to low-temperature nitridation that improved the corrosion resistance of austenite subgrains. Therefore, the etching solution cannot attack the austenite and it remains featureless.

Through the microscopic study it is evident that a nitrided layer is visible, and the layer thickness is dependent on the length of treatment time; showing greater thickness over a longer period. It can be seen that the thickness of the total nitrided layer is approximately 15 and 28 μm after salt nitriding treatment at 450 °C for 16 and 40 h, respectively. Figure 3 shows the thickness of the nitrided layer, as a function of salt bath time at 450 °C. In this case, it is showing a parabolic rate law with treatment time. This result suggested that this molten salt bath nitriding was controlled by a diffusion process.

3.2 Phase Analysis of the Nitrided Layer in DSS 2205

After removing the oxide film, probably Cr_2O_3 by gentle metallographic polishing, x-ray diffraction patterns of the untreated and nitrided samples were obtained, as shown in Fig. 4. A conventional diffraction pattern of untreated samples (labeled "untr" in figure) is shown for comparison. According to these patterns, it is obvious that the phase composition change of nitrided layers on SAE 2205 steel depends on nitriding time. The phases present in the untreated sample are dominated by austenite and ferrite. After salt bath nitriding treatment at 450 °C for 1-4 h, the phase composition of the sample has changed minimally. This minimal change implies that the intensity of the ferrite peaks has weakened. This weakness is most likely due to the diffusion of the N atom, which is an intensive austenitic forming element. When the ferrite in the nitrided layer supersaturates more N atoms from the molten salt medium, it assists in the formation of a mixture layer of austenite (F + [N] → A). After reaching a nitriding time at 450 °C for up to 8 h, there are identifiable peaks of the expanded austenite that start to form, which can also be called the "S phase" according to previous reports (Ref 5-7). The transformation can be included in the formula: (1) F + [N] → A → A_N and (2) A → A_N; A_N as the expanded austenite (S phase) by nitrogen; which also coincides with the microstructure observed. Meanwhile, some high-angle diffraction peaks of austenite and ferrite disappeared. This change is probably due to the gradient of nitrogen, residual stresses, and the defect structure of the nitrided layers (Ref 10). Moreover, no well-defined, sharp Bragg reflection peaks can be observed for low-temperature-treated samples in the nitrided 8 h sample.

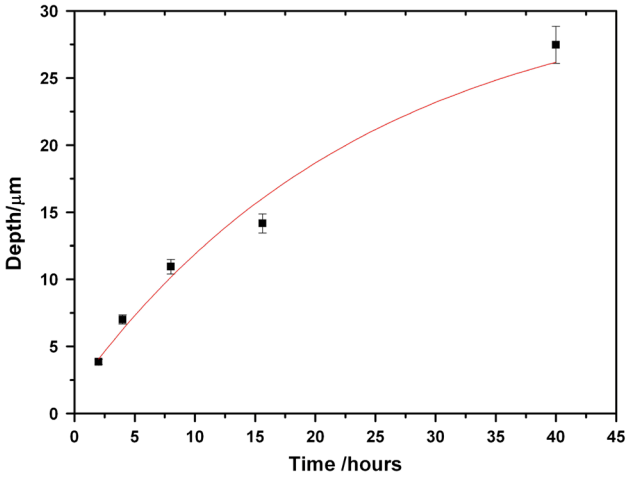

Fig. 3 The thickness of the nitrided layer versus processing time

When extending the time to 16 h, the peaks of ε-$Fe_{2-3}N$ start to appear and the peaks of the S phase become weakened, which indicated that the S phase produced by salt bath nitriding was transforming into the nitride. This transformation is undoubtedly due to the precipitation of nitride, which depletes the alloy elements of the expanded phase at 450 °C, favoring the formation of a mixture microstructure (S → A + ε-nitride) (Ref 17). By extending time to 40 h, the peaks of ε and CrN intensified and the peaks of the S phase were seriously weakened. In fact, the equilibrium solubility limit of nitrogen in ferritic structure is overly exceeded at 450 °C, which is where the precipitation of nitride occurs. In addition, a relatively stable nitride is much easier to form at 450 °C because nitride formation is aided by its high-negative enthalpy and low Cr diffusivity in the matrix at a temperature greater than 450 °C (Ref 18).

The microstructure of a nitrided layer of SAE 2205 stainless steel sample observed by TEM at a low magnification, as shown in Fig. 5, was obtained from an untreated specimen. The

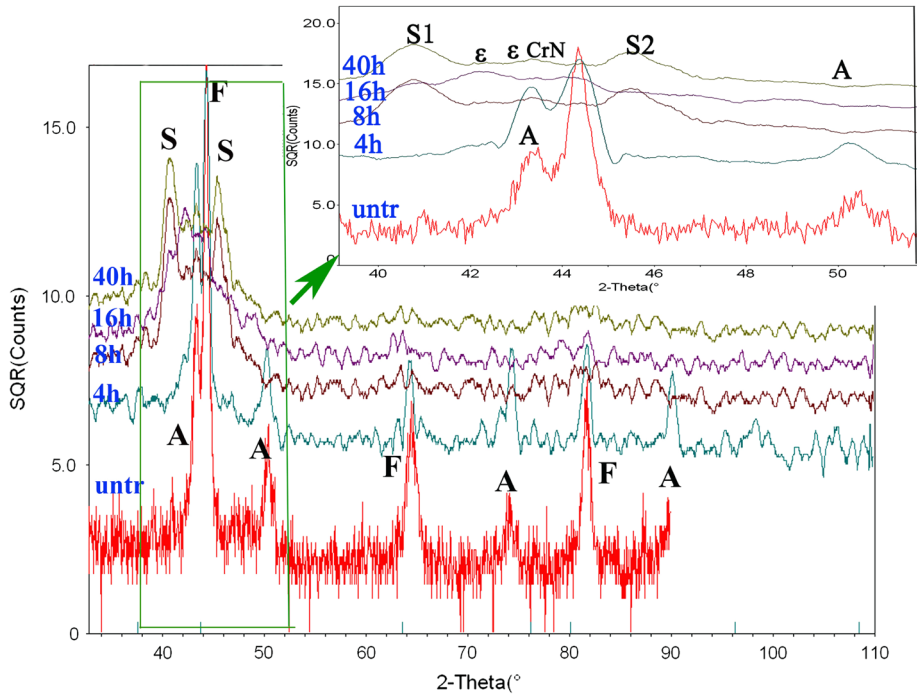

Fig. 4 XRD patterns of nitrided and unnitrided 2205 SS for different times (at 450 °C)

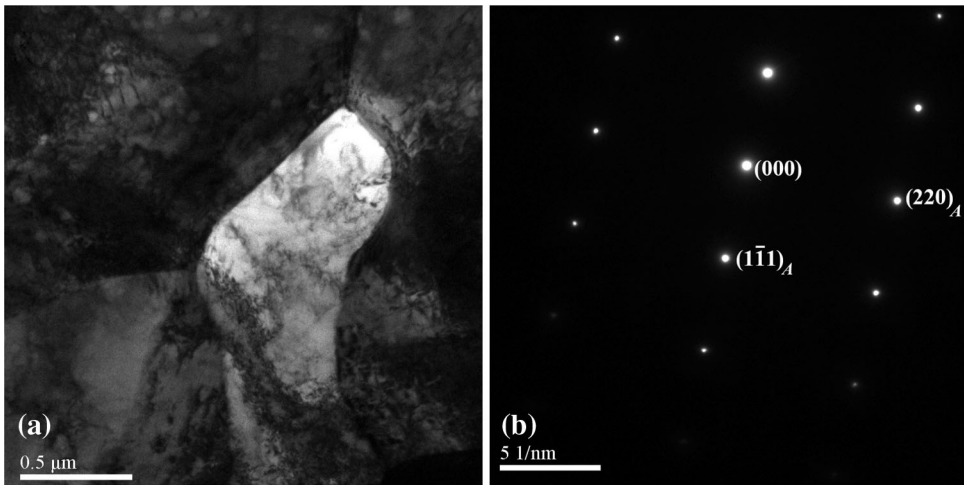

Fig. 5 Microstructure of the as-received SAE 2205 stainless steel (a typical duplex phase microstructure, b SADP of a)

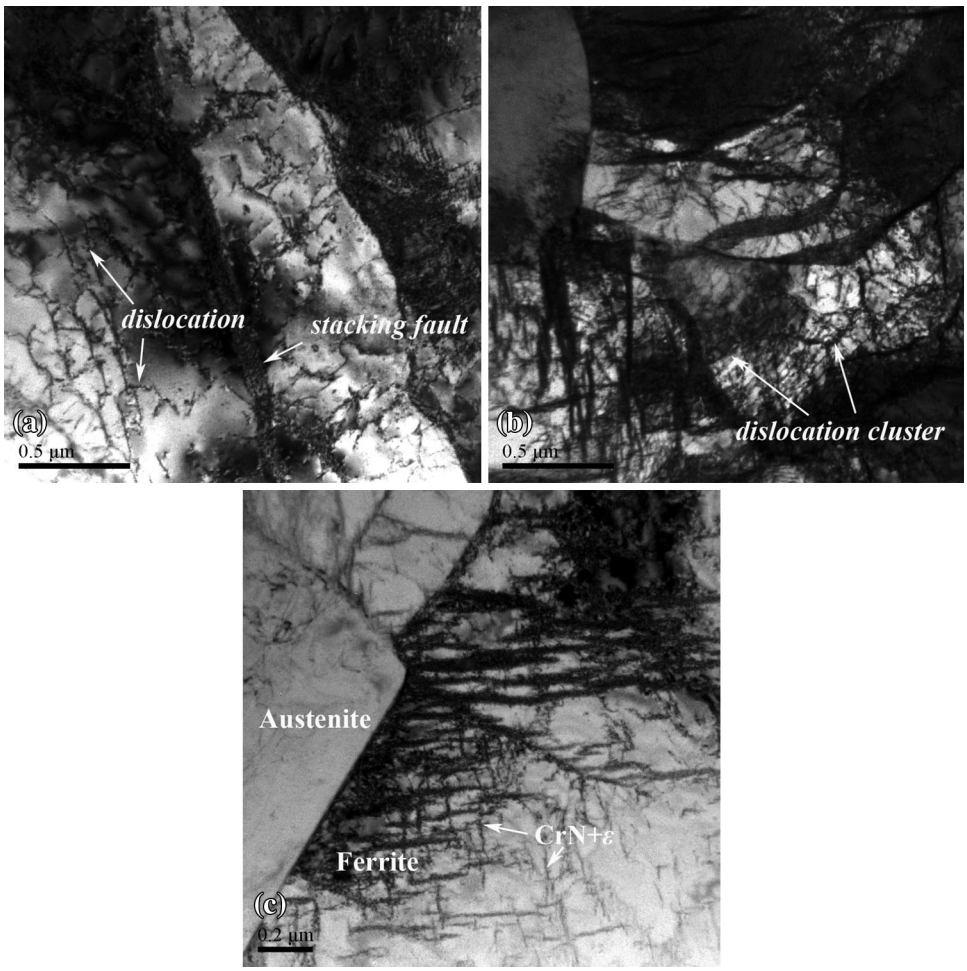

Fig. 6 Microstructure of SAE 2205 DSS salt bath nitrided for 40 h at 450 °C (a stacking fault and dislocation, b dislocation cluster, c nitride precipitate in ferrite zone)

corresponding microstructure was essentially composed of a duplex phase structure, label in Fig. 5a, which is consistent with the selected area diffraction pattern (SADP), as shown in Fig. 5b.

The typical microstructures of the modified layer of low-temperature salt bath nitriding 2205 stainless steel are shown in Fig. 6. According to Christiansen (Ref 3), there are multiple stacking faults and dislocation clusters caused by nitrogen atom

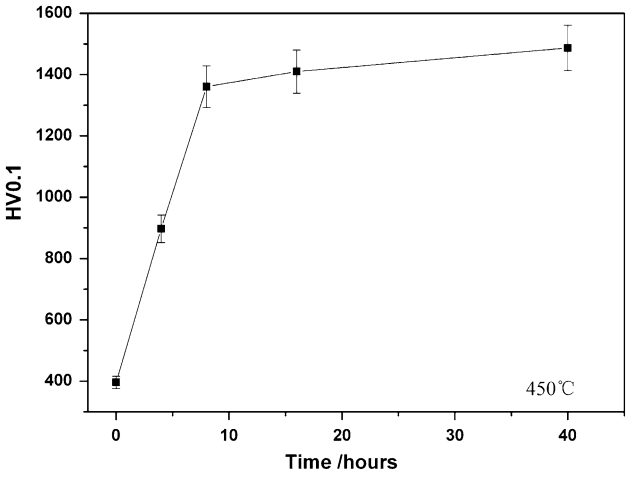

Fig. 7 Microhardness of SAE 2205 DSS salt bath nitrided for various times at 450 °C

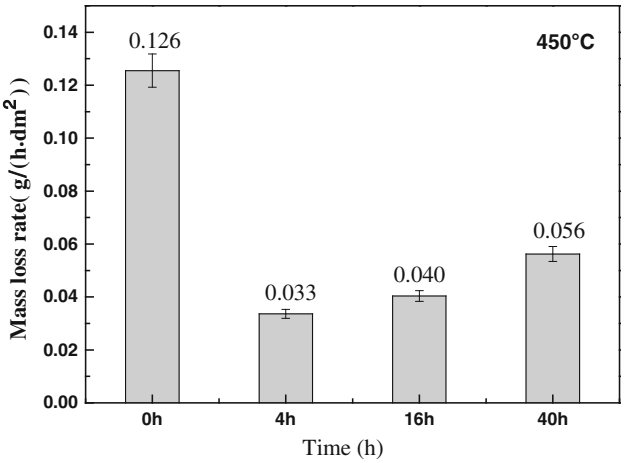

Fig. 8 Erosion/corrosion rate of various SAE 2205 stainless steels in 20 % H_2SO_4 two phases flow

diffusion. Both austenite and ferrite zones have plenty of stacking faults as well as dislocation (Fig. 6b), which is caused by N diffusion into the austenite and ferrite. However, looking from a different point of view (Fig. 6c), the nitride precipitate in ferrite zone can be observed with no precipitate in the austenite zone.

3.3 Hardness and Erosion/Corrosion Behavior

Figure 7 shows the microhardness of nitrided layers of salt bath nitride 2205 stainless steel as a function of time at 450 °C. As shown in the image, a very steep microhardness increase was found on the sample surface; which also came to a gradual level of stability when temperature rose at approximately the 4 h mark. The maximum values measured from the treated surface are estimated at 1400 $HV_{0.1}$ after 8 h, which is about 3.5 times as hard as the untreated material (396 HV0.1). The extremely high values of the microhardness can be explained by the large misfit-induced stress fields associated with the abundance of the dislocation groups and stacking faults, which was caused by the supersaturation of nitrogen in the solid solution. The higher surface hardness over a longer period of time (e.g. 40 h) was accompanied by the formation of a significant number of finely dispersed nitride phases, which have a precipitate-hardening effect.

Under the same condition, the ratio of erosion rate of the untreated sample can be seen in Fig. 8. Due to its relatively low hardness, the surface of the untreated sample was severely corroded during erosion testing. The surface SEM micrographs of the samples after erosion/corrosion are shown in Fig. 9. Many cutting scratches can be observed in the surface of the untreated sample, which is due to the low hardness surface of the stainless steel; as it was directly eroded by the corrosion of the dilute sulfuric acid solution and the impact of the Al_2O_3 grains (Fig. 9a). As for the nitrocarburized samples, the nitrocarburized layer formed at the surface of the stainless steel. The erosion happened at the hardening layer to protect the stainless steel, which can be viewed from the sample treated for 4 h (Fig. 9b). This sample shows relatively less eroded damage, nearly no cracks, and the eroded tracks on the surface layer were found to be relatively shallow and superficial. After long-term nitriding, the nitrides precipitated in the modified layer, and the corrosion resistance declined.

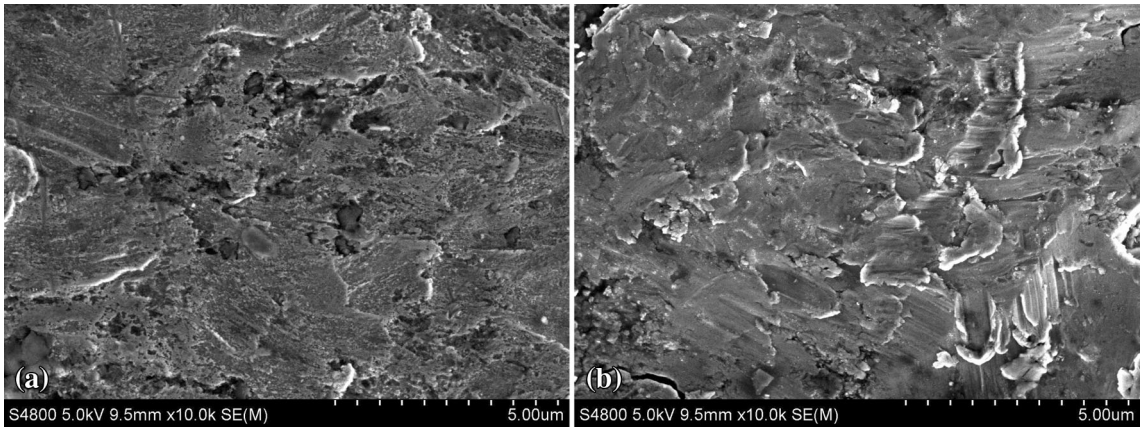

Fig. 9 SEM micrographs of the erosion-corrosioned samples (a untreated, b nitrocarburized for 4)

Compared with the untreated sample, both nitrided samples exhibited milder erosion damage and a lower erosion rate. The improvement of the erosion resistance for nitrided SAE 2205 stainless steel is considered a direct product of the combined effects on the microstructure, the high surface hardness, and the high compressive residual stress in the nitrided layer. The higher surface hardness can bear more stringent plastic deformation, and reduce the plough grooves and cutting damages impacted by particles (Ref 26, 27). The supersaturated nitrogen in the nitrided layer can introduce high compressive residual stresses (Ref 28, 29), which will tend to counteract a part of the kinetic energy of impact particles (Ref 6, 30). After treatment for 4 h, the modified layer of the stainless steel samples was the expanded austenite, which has better corrosion resistance and high microhardness (Ref 31). So the 4 h treated sample has the best erosion/corrosion behavior. After nitriding for 16 and 40 h, the brittle nitride decomposed in the modified layer and some cracks formed as the treated time prolonged. The decomposed modified layer cannot bear the impact in the corrosion environment. So the erosion/corrosion resistance decreased. Further investigations are needed to verify the mechanism(s) involved.

4. Conclusion

From the above-mentioned investigations, it may be concluded that when SAE 2205 duplex stainless steel is subjected to complex salt bathing nitrocarburizing at 450 °C, the following occur.

1. After 2205 stainless steel was subjected to salt bath nitriding at 450 °C for a period of time less than 8 h, the ferrite in the sample surface transformed into the austenite through active nitrogen diffusion, and the main phase of the modified layer generally expanded the austenite. When the treatment time was extended up to 16 h, the preexisting ferrite zone in the expanded austenite decomposed and transformed partially into ε-nitride precipitate. When the time was lengthened up to 40 h, the preexisting ferrite in the expanded austenite decomposed and transformed into ε-nitride and CrN precipitate.
2. An expanded austenite layer was formed on the surface of the substrate with a thickness changing from 3 to 28 μm over a gradual range of time. The growth of the thickness of the nitride layer was primarily controlled by the nitrogen diffusion, which is evident from the Parabolic Rate Law.
3. The salt bath nitrocarburizing can effectively improve the surface hardness of SAE 2205 stainless steel. The maximum values measured from the treated surface were observed to be approximately 1400 $HV_{0.1}$ for 8 h, which is about 3.5 times as hard as the untreated material (396 $HV_{0.1}$).
4. Low-temperature salt bath nitrocarburizing can improve the erosion/corrosion resistance against two phases of flow. After nitriding for 4 h, it can be concluded that the sample will have the best corrosion resistance.

Acknowledgments

The authors are very grateful to the National Natural Science Foundation of China (Grant No. 50901047) for financial support of the research and work involved in this study. Further acknowledgements should go to the author (J.W) along with Prof. *Baoluo Shen* of Sichuan University and Prof. *Defu Luo* of XiHua University, P.R.China, for their valuable discussions during the course of the research.

References

1. C. Blawert, A. Weisheit, B.L. Mordike, and F.M. Knoop, Plasma Immersion Ion Implantation of Stainless Steel: Austenitic Stainless Steel in Comparison to Austenitic-Ferritic Stainless Steel, *Surf. Coat. Technol.*, 1996, **85**, p 15–27
2. L.H. Chiu, Y.Y. Su, F.S. Chen, and H. Chang, Microstructure and Properties of Active Screen Plasma Nitrided Duplex Stainless Steel, *Mater. Manuf. Process.*, 2010, **25**, p 316–323
3. T.L. Christiansen and M.A.J. Somers, Controlled Dissolution of Colossal Quantities of Nitrogen in Stainless Steel, *Metall. Mater. Trans. A*, 2006, **37**, p 675
4. Y. Lin, J. Lu, L. Wang, T. Xu, and Q. Xue, Surface Nanocrystallization by Surface Mechanical Attrition Treatment and its Effect on Structure and Properties of Plasma Nitrided AISI, 321 Stainless Steel, *Acta Mater.*, 2006, **54**, p 5599–5605
5. T.S. Hummelshøj, T.L. Christiansen, and M.A.J. Somers, Lattice expansion of carbon-stabilized expanded austenite, *Scripta Mater.*, 2010, **63**, p 761–763
6. L. Wang, X. Bin, Y. Zhiwei, and S. Yaqin, The Wear and Corrosion Properties of Stainless Steel Nitrided by Low-Pressure Plasma-Arc Source Ion Nitriding at Low Temperatures, *Surf. Coat. Technol.*, 2000, **130**, p 304–308
7. L. Wang, S. Ji, and J. Sun, Effect of Nitriding Time on the Nitrided Layer of AISI, 304 Austenitic Stainless Steel, *Surf. Coat. Technol.*, 2006, **200**, p 5067–5070
8. R.B. Frandsen, T. Christiansen, and M.A.J. Somers, Simultaneous Surface Engineering and Bulk Hardening of Precipitation Hardening Stainless Steel, *Surf. Coat. Technol.*, 2006, **200**, p 5160
9. S. Sienz, S. Mandl, and B. Rauschenbach, In Situ Stress Measurements During Low-Energy Nitriding of Stainless Steel, *Surf. Coat. Technol.*, 2002, **156**, p 185–189
10. A.S. Hamdy, B. Marx, and D. Butt, Corrosion Behavior of Nitride Layer Obtained on AISI, 316L Stainless Steel via Simple Direct Nitridation Route at Low Temperature, *Mater. Chem. Phys.*, 2011, **126**, p 507–514
11. Y. Sun and E. Haruman, Effect of Carbon Addition on Low-Temperature Plasma Nitriding Characteristics of Austenitic Stainless Steel, *Vacuum*, 2006, **81**, p 114–119
12. H. Tsujimura, T. Goto, and Y. Ito, Surface Nitriding of SUS 304 Austenitic Stainless Steel by a Molten Salt Electrochemical Process, *J. Electrochem. Soc.*, 2004, **151D**, p 67–71
13. H. Tsujimura, T. Goto, and Y. Ito, Electrochemical formation and control of chromium nitride films in molten LiCl–KCl–Li_3N systems, *Electrochimica. Acta*, 2002, **47**, p 2725–2731
14. K. Funatani, Low-Temperature Salt Bath Nitriding of Steels, *Met. Sci. Heat Treat.*, 2004, **46**, p 277–281
15. J.W. Zhang, L.T. Lu, K. Shiozawa, W.N. Zhou, and W.H. Zhang, Effect of Nitrocarburizing and Post-Oxidation on Fatigue Behavior of 35CrMo Alloy Steel in Very High Cycle Fatigue Regime, *Int. J. Fatigue*, 2011, **33**, p 880–886
16. P. Jacquet, J.B. Coudert, and P. Lourdin, How Different Steel Grades React to a Salt Bath Nitrocarburizing and Post-Oxidation Process: Influence of Alloying Elements, *Surf. Coat. Technol.*, 2011, **205**, p 4064–4067
17. Y.Z. Shen, K.H. Oh, and D.N. Lee, Nitriding of Steel in Potassium Nitrate Salt Bath, *Scripta Mater.*, 2005, **53**, p 1345–1349
18. H. Tsujimura, T. Goto, and Y. Ito, Electrochemical Surface Nitriding of Pure Iron by Molten Salt Electrochemical Process, *J. Alloys Compd.*, 2004, **376**, p 246–250
19. H.Y. Li, D.F. Luo, C.F. Yeung, and K.H. Lau, Microstructural Studies of QPQ Complex Salt Bath Heat-Treated Steels, *J. Mater. Process. Technol.*, 1997, **69**, p 45
20. C.F. Yeung, K.H. Lau, H.Y. Li, and D.F. Luo, Advanced QPC Complex Salt Bath Heat Treatment, *J. Mater. Process. Technol.*, 1997, **66**, p 249
21. G.-J. Li, Q. Peng, J. Wang, C. Li, Y. Wang, J. Gao, S.-Y. Chen, and B.-L. Shen, Surface Microstructure of 316L Austenitic Stainless Steel

by the Salt Bath nitrocarburizing and Post-Oxidation Process Known as QPQ, *Surf. Coat. Technol.*, 2008, **202**, p 2865–2870

22. C.E. Foerster, F.C. Serbena, S.L.R. da Silva, C.M. Lepienski, CJdeM Siqueira, and M. Ueda, Mechanical and Tribological Properties of AISI, 304 Stainless Steel Nitrided by Glow Discharge Compared to Ion Implantation and Plasma Immersion Ion Implantation, *Nucl. Instr. Meth. B*, 2007, **257**, p 732
23. L.C. Gontijo, R. Machado, E.J. Miola, L.C. Casteletti, N.G. Alcantara, and P.A.P. Nascente, Study of the S Phase Formed on Plasma-Nitrided AISI, 316L Stainless Steel, *Mater. Sci. Eng. A*, 2006, **431**, p 315–321
24. J. Wang, Y. Lin, J. Yan, D. Zen, Q. Zhang, R. Huang, and H. Fan, Influence of Time on the Microstructure of AISI, 321 Austenitic Stainless Steel in Salt Bath Nitriding, *Surf. Coat. Technol.*, 2012, **206**, p 3399–3404
25. J. Wang, Y. Lin, J. Yan, D. Zen, R. Huang, and H. Zejing, Modification of AISI, 304 Stainless Steel Surface by the Low Temperature Complex Salt Bath Nitriding at 430°C, *ISIJ Int.*, 2012, **52**, p 1128–1133
26. D. Lopez, C. Sanchez, and A. Toro, Corrosion-Erosion Behavior of TiN-Coated Stainless Steels in Aqueous Slurries, *Wear*, 2005, **258**, p 684–692
27. S.D. Chyou and H.C. Shih, The Effect of Nitrogen on the Corrosion of Plasma-Nitrided 4140 Steel, *Corrosion*, 1991, **47**(1), p 31–34
28. C.X. Li and T. Bell, Corrosion Properties of Active Screen Plasma Nitrided 316 Austenitic Stainless Steel, *Corros. Sci.*, 2004, **46**, p 1527–1547
29. E. Menthe and K.-T. Rie, Further Investigation of the Structure and Properties of Austenitic Stainless Steel After Plasma Nitriding, *Surf. Coat. Technol.*, 1999, **116–119**, p 199
30. K.C. Chen, J.L. He, W.H. Huang, and T.T. Yeh, Study on the Solid–Liquid Erosion Resistance of Ion-Nitrided Metal, *Wear*, 2002, **252**, p 580–585
31. H. Dong, S-Phase Surface Engineering of Fe–Cr, Co–Cr and Ni–Cr Alloys, *Int. Mater. Rev.*, 2010, **55**(2), p 65–98